Journal of Magnetic Resonance **148,** 11–22 (2001)
doi:10.1006/jmre.2000.2233, available online at http://www.idealibrary.com on IDEAL®

A Faster Way to Characterize by Triple-Quantum-Filtered ^{17}O NMR Water Molecules Strongly Bound to Macromolecules in Solution

Alexandre Lehoux, Maciej Krzystyniak,* and Evelyne Baguet[1]

*Laboratoire d'analyse isotopique et électrochimique de métabolismes, UPRES-A CNRS 6006, Université de Nantes, BP 92208, 2 rue de la Houssinière, F-44322 Nantes cedex 03, France; and *Institute of Physics, Jagiellonian University, Reymonta 4, 30-059 Krakow, Poland*

Received February 29, 2000; revised September 18, 2000

The simultaneous use of transverse and longitudinal relaxation rates, together with a transverse triple-quantum-filtering NMR sequence, was estimated for the adequate characterization of ^{17}O-water relaxation behavior in protein solutions. A complementary contribution to transverse relaxation was found, which was interpreted as chemical exchange of ^{17}O-water between different sites of the proteins. This contribution was estimated via calibration measurements. Then, for other similar samples, faster experiments could be performed. The analysis of the results obtained in this way gave adequate values of the relaxation rate of water in fast motion, of the fraction of water in slow motion, and of its correlation time. Hence, it permitted the complete characterization of the sample in a reasonable experimental time.

Key Words: **lysozyme; NMR, ^{17}O-water; buried water; quadrupolar relaxation; triple-quantum-filtered spectra.**

INTRODUCTION

The water–protein interaction has long been recognized as a major determinant of chain folding, conformational stability, internal dynamics, and binding specificity of globular proteins (*1, 2*). In recent years, the study of water/protein systems by various NMR techniques has led to a better understanding of water behavior in the presence of proteins. Different ways of analyzing the hydration have been developed. A few specific hydration molecules of low mobility were detected on small proteins by ^1H NOE techniques (*3*). The simultaneous study of water ^{17}O and deuterium longitudinal relaxation dispersion at different field strengths enabled the estimation of the fraction of water in slow motion and its mobility (*4–6*). Comparable results were obtained via ^1H NMR in dilute samples (*7*). Also, the study, via triple-quantum-filtering sequences, of $H_2{}^{17}O$ multiexponential behavior in the presence of biological macromolecules enabled the detection of strongly bound or buried water (*8–12*). This last method has the advantage over relaxation-dispersion measurements in that it does not require experiments to be performed at a wide range of magnetic field strengths. Also, if both transverse and longitudinal relaxation are studied with triple-quantum-filtered sequences, the method allows an independent determination of the number of strongly bound water molecules and of their average correlation time (*8*). It can also be used to determine the mobility and the number of water molecules trapped in a protein–inhibitor complex, whatever its size, contrary to ^1H NOE techniques. Results obtained in this way are consistent with those obtained by other methods. Unfortunately, as the longitudinal triple-quantum-filtered signal is particularly small, the measurement can be very time consuming, particularly for samples in which the ^{17}O is at natural abundance or only slightly enriched. It would be particularly interesting to develop a faster method, so as to enable the study of biological samples where enrichment is impossible, or when a rapid measurement is required.

The apparent transverse relaxation time of water contains information about the mobility and fraction of water in slow motion, as does its longitudinal relaxation time (*5*). These two relaxation times have been used at different field strengths to characterize the hydration of proteins (*13, 14*). But then, the correlation time of water interacting with lysozyme was different when T_1 and T_2 of ^{17}O-water were analyzed (*14*) from when T_1 only of water was analyzed by both ^{17}O and deuterium NMR (*6*). This was explained by the existence of a supplementary contribution to T_2 of ^{17}O-water, corresponding to scalar relaxation of the first kind (*5*). Despite this contribution, one may wonder whether the information the transverse relaxation time of ^{17}O-water brings could still replace those of the longitudinal triple-quantum-filtered experiment, for the ^{17}O NMR analysis of water at one field strength.

This paper reports the use of transversal triple-quantum-filtering pulse sequences together with standard (longitudinal and transverse) relaxation measurements, to determine the number of water molecules in slow motion per protein, their correlation time, and the relaxation rate of water in fast motion.

First, basic principles of quadrupolar relaxation and chemical exchange are applied to ^{17}O-water relaxation. Then, the possibility of deducing univocally the fraction and correlation time of water in slow motion from measurements at one field strength from transverse and longitudinal relaxation times to-

[1] To whom correspondence should be addressed. Fax: +33 (0)2 51 12 57 12. E-mail: Evelyne.Baguet@chimbio.univ-nantes.fr.

1090-7807/01 $35.00

gether with the transverse triple-quantum-filtered (TQF) signal is estimated. Finally, the validity of standard T_2 measurements by Hahn echoes is estimated, for the characterization of water interacting with protein mobility. For that, different protein solutions of bovine serum albumin and hen egg white lysozyme are studied via a method already validated: the study of longitudinal and transverse TQF signals together with longitudinal relaxation, from which the desired parameters—the relaxation rate of water in fast motion, the correlation time, and the fraction of water in slow motion—are deduced. From these results, a theoretical value of the water transverse relaxation rate is estimated, which is compared to the measured relaxation rate of water. After that, a sample, where the transverse TQF signal and the transverse and longitudinal relaxation are measured, is studied. The parameters concerning water in slow and fast lotion are estimated, together with their precision.

THEORY

I. Basic Principles

Two phenomena play a key role in ^{17}O-water relaxation in the presence of proteins: the quadrupolar relaxation of water in the different states with various mobilities and the chemical exchange between these states. The quadrupolar relaxation of water in an isotropic system will be first described as a function of the mobility of nuclei. We will then describe chemical exchange between the different sites and its consequences upon the time course of magnetization.

a. Relaxation of ^{17}O-Water in the Presence of Proteins

The NMR relaxation behavior of quadrupolar nuclei, such as ^{17}O in water, is best described by using the irreducible tensor operator formalism (*15, 16*). In this basis set, the density matrix $\sigma(t)$ is decomposed to give

$$\sigma(t) = \sum_{l=0}^{2I} \sum_{p=-l}^{l} b_{l,p}(t) T_{l,p}, \qquad [1]$$

where l is the rank of the operator, which describes the complexity (number of eigenstates) of the system, and p is its coherence order. In this new basis, and for uncoupled spins, the components of odd and even rank vary independently. The initial state of the magnetization for relaxation measurements is $-S_z$ and S_x for longitudinal and transverse relaxation, respectively. In the irreducible tensor basis set, these operators can be decomposed to give

$$S_x = \frac{\sqrt{35}}{2}(T_{1,-1} - T_{1,+1}) \quad \text{and} \quad -S_z = -\frac{\sqrt{70}}{2} T_{1,0}. \qquad [2]$$

As the rank of these operators is one, and we assume that there is no quadrupolar splitting, only odd ranks of $T_{l,p}$ will appear during the magnetization relaxation. Then, it is possible to study only the components of $\sigma(t)$ which have odd rank, so as to describe the time course of magnetization.

The free precession of the magnetization does not modify the order p of the irreducible operators. So, when the transverse magnetization is studied, the density matrix is the sum of the $T_{l,p}$ terms with $p = \pm 1$. For reasons of symmetry, it is sufficient to determine the coefficients for $p = \pm 1$. The only part of $\sigma(t)$ one needs to study is then

$$\sigma_{\text{odd}}^{p=+1}(t) = \{b_{11}^{(1)}(t),\ b_{31}^{(1)}(t),\ b_{51}^{(1)}(t)\}. \qquad [3]$$

Its time evolution is given by

$$\frac{d}{dt}\sigma_{\text{odd}}^{p=+1}(t) = -\mathbf{R'}^{(1)}\sigma_{\text{odd}}^{p=+1}(t), \qquad [4]$$

where $\mathbf{R'}^{(1)}$ is the Redfield matrix for pure quadrupolar relaxation of single-quantum coherences with odd rank, expressed in the irreducible operator basis (*16*),

$$\mathbf{R'}^{(1)} = K\begin{bmatrix} A' & D' & 0 \\ D' & B' & E' \\ 0 & E' & C' \end{bmatrix}, \qquad [5]$$

with the elements

$$\begin{cases} A' = \dfrac{16}{5}(3J_0 + 5J_1 + 2J_2), & D' = \dfrac{216}{5\sqrt{21}}(J_0 - J_2) \\ B' = \dfrac{2}{15}(123J_0 + 370J_1 + 497J_2), & E' = \dfrac{20}{3\sqrt{14}}(3J_0 + 14J_1 - 17J_2) \\ C' = \dfrac{4}{3}(3J_0 + 26J_1 + 16J_2) \\ K = \dfrac{3}{8000}\left(\dfrac{e^2qQ}{\hbar}\right)^2\left(1 + \dfrac{\eta^2}{3}\right) \end{cases} \qquad [6]$$

and the spectral densities for isotropic motion, $J_n = 2\tau_c/(1 + (n\omega_0\tau_c)^2)$.

In the inversion-recovery experiment, the order of the coherence will be $p = 0$ after the initial inverting pulse. So, to determine the magnetization time course, one only needs to determine the density operator $\Delta\sigma^{p=0}_{\text{odd}}(t) = \sigma^{p=0}_{\text{odd}}(t) - \sigma^{p=0}_{\text{odd}}|_{\text{eq}} = \{\Delta b^{(0)}_{1,0}, \Delta b^{(0)}_{3,0}, \Delta b^{(0)}_{5,0}\}$ which is given by the relation

$$\frac{d}{dt}\Delta\sigma^{p=0}_{\text{odd}}(t) = -\mathbf{R}'^{(0)}\Delta\sigma^{p=0}_{\text{odd}}(t). \qquad [7]$$

Here again, $\mathbf{R}'^{(0)}$ is the Redfield relaxation matrix with odd rank, expressed in the irreducible operator basis (*16*),

$$\mathbf{R}'^{(0)} = K\begin{bmatrix} P' & S' & 0 \\ S' & Q' & T' \\ 0 & T' & R' \end{bmatrix}, \qquad [8]$$

with the elements

$$\begin{cases} P' = \dfrac{32}{5}(J_1 + 4J_2), & S' = \dfrac{144}{5}\sqrt{\dfrac{2}{7}}(J_1 - J_2) \\ Q' = \dfrac{4}{5}(82J_1 + 83J_2), & T = 40\sqrt{\dfrac{5}{7}}(J_1 - J_2) \\ R' = 20(2J_1 + J_2). \end{cases} \qquad [9]$$

In this basis set, the relaxation matrices $\mathbf{R}'^{(0)}$ and $\mathbf{R}'^{(1)}$ of water in fast motion, for which $\omega_0\tau_c \ll 1$, may be obtained by replacing J_n by $2\tau_c$. They are then diagonal, with the diagonal terms equal to R_{bulk}, (33/8) R_{bulk}, and (15/8) R_{bulk}, which correspond to the relaxation rates of the single-, triple-, and fifth-quantum coherences, respectively. These matrices are called $\mathbf{R}_{\text{bulk}}$.

b. Fast Chemical Exchange between the Different Types of Water

Consider first the simple case where there is chemical exchange between two populations A and B whose magnetizations evolve exponentially. The fractions of A and B are called p_A and p_B, respectively; their transverse relaxation rates in the absence of chemical exchange are R_{2A} and R_{2B}, respectively, whereas k_A and k_B are the unidirectional rates of transformation of A to B and B to A, respectively. A is on resonance and the chemical shift of B is $\Delta\omega$. It is assumed that $R_{2A} < R_{2B}$ and $p_A > p_B$. To determine the lineshapes of A and B in the presence of chemical exchange, it is sufficient to find the roots of the matrix (*17*)

$$\begin{bmatrix} R_{2A} + k_A & -k_B \\ -k_A & R_{2B} + k_B + i\Delta\omega \end{bmatrix}. \qquad [10]$$

They are

$$\lambda_{\pm} = \frac{R_{2A} + k_A + R_{2B} + k_B + i\Delta\omega}{2} \mp \left(\frac{(R_{2A} + k_A + R_{2B} + k_B + i\Delta\omega)^2}{4} - (R_{2A} + k_A)(R_{2B} + k_B) + k_Ak_B - i\Delta\omega(R_{2A} + k_A)\right)^{1/2}. \qquad [11]$$

When the chemical exchange is slow, the real and imaginary parts of λ_+ correspond to the relaxation rate and frequency of A whereas λ_- characterizes B. When the chemical exchange becomes faster, the two peaks approach one another, until λ_+ reaches the weighted mean frequency (*18*),

$$\bar{\omega} = \omega_A p_A + \omega_B p_B = \Delta\omega p_B, \qquad [12]$$

and its real part is equal to

$$\bar{R}_2 = p_A R_{2A} + p_B R_{2B}. \qquad [13]$$

At the same time, the other solution λ_- has a chemical shift symmetrical to $\bar{\omega}$ with respect to the average $\Delta\omega/2$ and its real part becomes very large, finally not corresponding to a physical solution anymore. In the intermediate state, that is, when $\Delta\omega/k_B$ cannot be neglected compared to 1, the value of λ_+ also depends on $\Delta\omega$ and k_B. Of course, Eqs. [12] and [13] are no longer valid. On the contrary, the longitudinal relaxation rate is still the weighted average of A and B longitudinal relaxation rates.

For a quadrupolar spin system with several states undergoing fast exchange, the relaxation matrix for a given coherence n obeys an equation similar to Eq. [13] (*19*). This is formally expressed by

$$\mathbf{R}^{(n)}_{\text{water}} = \sum_i p_i\mathbf{R}^{(n)}_i, \qquad [14]$$

where $\mathbf{R}^{(n)}_i$ is the relaxation matrix for state i in the absence of exchange and $\mathbf{R}^{(n)}_{\text{water}}$ is the global relaxation matrix of water in exchange between the different states. These states can be divided into two groups, water in fast motion, which obeys the relationship $\omega_0\tau_c \ll 1$ and for which the relaxation matrices $\mathbf{R}^{(n)}_i$ are diagonal, and water in slow motion, whose transverse and longitudinal relaxation can be described by the 3×3 relaxation matrices given in Eqs. [5]–[6] and [8]–[9]. Then, all water in fast motion (free water and water in small interactions with the proteins in solutions) can be described by a global relaxation matrix $\mathbf{R}_{\text{bulk}}$, which is fully described by the relaxation rate R_{bulk}, the average relaxation rate of water in fast

motion. If the different types of water in slow motion have a close correlation time, whose average value will be called τ_s, it is also possible to consider their global relaxation matrices $\mathbf{R}_S^{(n)}$ whose values are given in Eqs. [5]–[6] and [8]–[9] where the generic name τ_c is replaced by τ_s. The global relaxation matrices of water are then

$$\mathbf{R}_{\text{water}}^{(n)} = p_s \mathbf{R}_s^{(n)} + (1 - p_s)\mathbf{R}_{\text{bulk}}, \qquad [15]$$

where n is equal to 0 or 1 for longitudinal or transverse magnetization, respectively, and p_s is the fraction of water in slow motion.

One should note that Eq. [15] is also only valid if the chemical exchange is fast enough, that is, if (1) the exchange between water in slow and fast motion and (2) the exchange between the different types of water in fast motion (i.e., free water and surface water weakly interacting with the protein) are fast enough compared with the difference of chemical shift between the sites in exchange. The case in which there would be exchange that was not fast enough between different types of water molecules in slow motion is less probable. In lysozyme, these water molecules, which correspond to buried water, are very few, about 4 (*20, 21*). If there were an accelerated decrease of the magnetization because of chemical exchange between them, this magnetization would collapse rapidly and multiexponential relaxation of water could hardly be detected (*16*).

c. Characterization of Water Properties

For given values of p_s and τ_s, the time course of the longitudinal and transverse magnetizations can be determined by diagonalizing numerically the relaxation matrices $\mathbf{R}_{\text{water}}^{(n)}$, which permits the calculation of the components of the matrix $\mathbf{f}^{(n)}(t) = \exp(-\mathbf{R}_{\text{water}}^{(n)}t)$. The functions $f_{l'l}^{(n)}(t)$, which compose each matrix $\mathbf{f}^{(n)}$, can be written (*16, 8*)

$$f_{l'l}^{(n)}(t) = \sum_{q=\text{I}}^{\text{III}} a_{l'l,q}^{(n)} \exp(-R_q^{(n)}t), \qquad [16]$$

with the relaxation rates $R_{\text{I}}^{(n)}$, $R_{\text{II}}^{(n)}$, and $R_{\text{III}}^{(n)}$ classified in increasing order. Usual pulse sequences, such as a single 90° pulse–acquire sequence, or spin echo and inversion-recovery sequences, access only the functions $f_{11}^{(n)}(t)$. In protein aqueous solutions, the fraction of water in slow motion is very small for the concentrations studied (*8*). Under these conditions, the off-diagonal terms of the relaxation matrix $\mathbf{R}_{\text{water}}^{(n)}$ can, as a "good" approximation, be neglected compared with the on-diagonal terms; the longitudinal and transverse magnetizations of water evolve almost monoexponentially. This means that for the functions $f_{11}^{(n)}(t)$, the coefficient $a_{11,\text{I}}^{(n)}$ is close to 1, whereas the two others, $a_{11,\text{II}}^{(n)}$ and $a_{11,\text{III}}^{(n)}$, are close to zero. Then, the longitudinal relaxation rate constant obtained after an inversion-recovery pulse sequence can be determined approximately by a perturbation treatment (*22*). It is equal to

$$R_{\text{I}}^{(0)} \cong p_s K \tfrac{32}{5}(J_1 + 4J_2) + (1 - p_s)R_{\text{bulk}}, \qquad [17]$$

whereas the transverse magnetization relaxation rate detected after a T_2 measurement is approximately

$$R_{\text{I}}^{(1)} \cong p_s K \tfrac{16}{5}(3J_0 + 5J_1 + 2J_2) + (1 - p_s)R_{\text{bulk}}. \qquad [18]$$

The relaxation rates $R_{\text{II}}^{(n)}$ and $R_{\text{III}}^{(n)}$ are more easily deducted from the study of the functions $f_{31}^{(n)}(t)$ and $f_{51}^{(n)}(t)$, themselves obtained by applying, at the end of the evolution time, a succession of pulses which constitutes a multiple-quantum filter (*23*). The function $f_{31}^{(1)}(t)$, for a spin $I = \frac{5}{2}$, can be studied selectively via the pulse sequence

$$90^\circ_\phi\text{–}\tau_e/2\text{–}180^\circ_\phi\text{–}\tau_e/2\text{–}70.5^\circ_{\phi+90}\text{–}\tau_m\text{–}90^\circ_0\text{–Acq.}(t_2), \qquad [19]$$

with ϕ chosen to select the desired multiple-quantum order (*15*). In the same way, the function $f_{31}^{(0)}(t)$ can be deduced from the measurements via the pulse sequence

$$180^\circ_0\text{–}\tau_e\text{–}70.5^\circ_\phi\text{–}90^\circ_0\text{–Acq.}(t_2). \qquad [20]$$

With the same approximations done as previously, the functions $f_{31}^{(n)}(t)$ are almost biexponentials, with the relaxation rates $R_{\text{I}}^{(n)}$ and $R_{\text{III}}^{(n)}$. The relaxation rates $R_{\text{III}}^{(n)}$ are given by

$$R_{\text{III}}^{(0)} \cong p_s K \tfrac{4}{5}(82J_1 + 83J_2) + (1 - p_s)\tfrac{33}{8}R_{\text{bulk}} \qquad [21a]$$

$$R_{\text{III}}^{(1)} \cong p_s K \tfrac{2}{15}(123J_0 + 370J_1 + 497J_2) + (1 - p_s)\tfrac{33}{8}R_{\text{bulk}} \qquad [21b]$$

and the coefficients $a_{31,\text{I}}^{(n)}$ and $a_{31,\text{III}}^{(n)}$ are equal to

$$a_{31,\text{I}}^{(0)} \cong -a_{31,\text{III}}^{(0)} = p_s K \frac{144}{5}\sqrt{\frac{2}{7}}\frac{J_1 - J_2}{R_{\text{I}}^{(0)} - R_{\text{III}}^{(0)}} \qquad [22a]$$

$$a_{31,\text{I}}^{(1)} \cong -a_{31,\text{III}}^{(1)} = p_s K \frac{216}{5\sqrt{21}}\frac{J_0 - J_2}{R_{\text{I}}^{(1)} - R_{\text{III}}^{(1)}}. \qquad [22b]$$

The signals obtained after triple-quantum filters are much smaller than those obtained in single-quantum experiments. But, they are still larger than the signals obtained after fifth-quantum filters, which are almost impossible to detect in a reasonable time for the samples considered.

At first sight, four experimental values characterizing the relaxation behavior of water in the presence of macromolecules can be studied easily for determining its characteristic parameters p_s, τ_s, and R_{bulk}. They are the relaxation rates $R_{\text{I}}^{(0)}$ and $R_{\text{I}}^{(1)}$

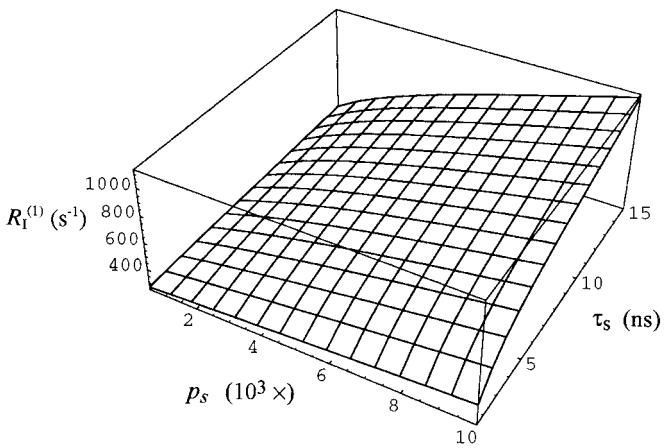

FIG. 1. Simulation of the transverse relaxation rate $R_I^{(1)}$ of ^{17}O-water in exchange between two populations in slow and fast motion for a given value of the longitudinal relaxation rate $R_I^{(0)}$, as a function of p_s and τ_s, the fraction and correlation time of water in slow motion.

and the signals of coherences 0 and 1 detected after triple-quantum-filtered sequences. The questions addressed are now the following: can one employ the parameter $R_I^{(1)}$ instead of the longitudinal TQF signal to characterize water behavior and does this give adequate results? If possible, this would be particularly interesting for saving time. The first question can be answered by simulations whereas the second one needs samples to be analyzed, which will be performed in the next part.

II. Unicity of the Solution

The aim is to determine whether a single pair of values of p_s and τ_s fits the experimental values of $R_I^{(1)}$ and of the signal detected after a transverse TQF sequence for a given sample where $R_I^{(0)}$ is known. For that, simulations of the relaxation rate $R_I^{(1)}$ and of the signal detected after a transverse triple-quantum filter are performed as a function of p_s and τ_s, for a given value of $R_I^{(0)}$. For given values of p_s and τ_s, R_{bulk} is deduced from $R_I^{(0)}$ (Eq. [17]), which is set to 260 s^{-1}, a value in the range of those found experimentally for various samples. All numerical values, except the unknown p_s and τ_s, are chosen the same as for a typical experiment. The values of $R_I^{(1)}$ and of the signal detected after a transverse triple-quantum filter are then deduced from Eqs. [18], [21b], and [22b]. The maximal amplitude in the time domain of the signal detected after a transverse TQF experiment is obtained at $t_{max}^{(1)}$ and for $\tau_e = t_{max}^{(1)}$, where $t_{max}^{(1)} = (\ln(R_I^{(1)}) - \ln(R_{III}^{(1)}))/(R_I^{(1)} - R_{III}^{(1)})$. Its simulation has already been represented in (*24*) for various values of p_s and τ_s. The signal increases with both p_s and τ_s in the range studied (p_s between 0.5 and 10% and τ_s between 1.5 and 15 ns). The value of the relaxation rate $R_I^{(1)}$ is simulated in the same way (Fig. 1). It also increases with both p_s and τ_s in the range studied. However, no direct conclusion can be given concerning the unicity of the solution. To obtain this assertion, the contour plots of the two simulation curves are drawn in Fig. 2. One can see that for the simulation of each experiment, after a transverse triple-quantum filter (dashed line) or for an apparent transverse relaxation rate measurement (straight line), a given value corresponds to many different pairs of values of p_s and τ_s. This confirms the results already obtained in (*10*). At the same time, one can see that two curves corresponding to the transverse relaxation rate of water and to the signal after transverse triple-quantum filters do not cross each other more than once. This means that for a given pair of values, there is no more than one pair of p_s and τ_s which corresponds to the exact solution.

These simulations have been repeated for various values of $R_I^{(0)}$ between 170 and 385 s^{-1}, the extreme limits found for the different samples studied. Curves similar to the one of Fig. 2 were found in all cases. From these simulations, one can conclude that a unique pair of values of p_s and τ_s does fit the data of the different samples studied in this work. Then, it is possible to deduce p_s and τ_s from the values of $R_I^{(0)}$ and $R_I^{(1)}$ and from the transverse triple-quantum-filtered experiment.

III. Limitations of the Approximations Made

For easiness, it was assumed in these simulations that the transverse and longitudinal signals of water evolved monoexponentially and that the transverse TQF signals evolved biexponentially. These approximations involve small systematic errors on the numerical values, especially for the signal detected after the triple-quantum filter, but without modifying their behavior significantly. Whereas it is sufficient for a qualitative study, it is not for a precise analysis of the transverse TQF signal. Then, this signal will be analyzed thereafter as a sum of three exponentials, from a numerical diagonalization of

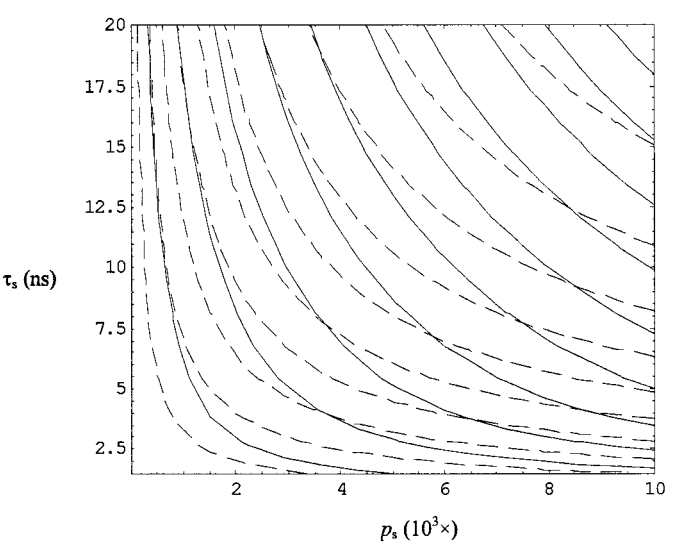

FIG. 2. Contour plot of the maximal transverse triple-quantum-filtered (TQF) signal of ^{17}O-water (- - -) and the transverse relaxation rate $R_I^{(1)}$ (—) of ^{17}O-water in exchange between two populations in slow and fast motion. The conditions are the same as those for Fig. 1.

the 3×3 relaxation matrix $\mathbf{R}^{(1)}_{\text{water}}$, as in previous publications (*8*, *9*, *24*). Also, the signal detected after a one-pulse sequence will be considered biexponential, neglecting the smaller term $a^{(1)}_{11,II}\exp(-R^{(1)}_{II}t)$. Hence, the approximate formula of the relaxation rates $R^{(1)}_{I}$ and $R^{(1)}_{III}$ will be obtained by diagonalization of the 2×2 reduced relaxation matrix of water $\{\{A', D'\}, \{D', B'\}\}$. In this way, and by replacing the relaxation rate R_{bulk} by the function of $R^{(0)}_{I}$, τ_s and p_s deduced from Eq. [17], the approximate value of $R^{(1)}_{I}$ is

$$R^{(1)}_{I} = \frac{1}{16}\,(8Ap_s + 8Bp_s - 41Pp_s + 41R^{(0)}_{I} - \sqrt{C}) \quad [23a]$$

with

$$C = 16(4A^2 - 8AB + 4B^2 + 16D^2 + 25AP)\,p_s^2 + 50(-8A + 8B - 25P)\,p_s R^{(0)}_{I} + 625(R^{(0)}_{I})^2$$

$$A = \frac{16}{5}\,K(3J_0 + 5J_1 + 2J_2),$$

$$B = \frac{2}{15}\,K(123J_0 + 370J_1 + 497J_2),$$

$$D = \frac{216}{5\sqrt{21}}\,K(J_0 - J_2),$$

$$P = \frac{32}{5}\,K(J_1 + 4J_2). \quad [23b]$$

This formula is quite more complicated than that given in Eq. [18] but should describe water transverse relaxation more precisely.

IV. Characterization of Hydration Water Properties from the Values $R^{(0)}_{I}$ and $R^{(1)}_{I}$ and from the Transverse TQF Signal

A program has been developed with Mathematica 3.0, which enables the relaxation rate of water in fast motion and the fraction and correlation time of water in slow motion to be deduced from the average ^{17}O relaxation rates $R^{(0)}_{I}$ and $R^{(1)}_{I}$ and the transverse TQF signal of water. Its principle is as follow. First, the signal of water after a one-pulse sequence is supposed as biexponential, with the relaxation rates $R^{(1)}_{I}$ and $R^{(1)}_{III}$ and the correlation time τ_s set to a given value. The equality between $R^{(1)}_{I}$, whose formula is given in Eqs. [23], and its experimental value is resolved numerically, which enables the determination of p_s, the fraction of water in slow motion. The relaxation rate R_{bulk} of water in fast motion is then calculated, and so are the signal detected after a transverse triple-quantum filter and the parameter χ^2, designed to estimate the closeness of the calculated signal to the one effectively detected. The value of τ_s is then optimized, so as to minimize χ^2.

EXPERIMENTAL

Hen egg white lysozyme, of activity about 70,000 units/mg, was obtained from Fluka (L'Isle d'Abeau, France) and bovine serum albumin (BSA), fraction V, of purity >96%, from Sigma Aldrich (L'Isle d'Abeau, France). Deuterated water at 99.9% and $H_2{}^{17}O$ at 10% were from Eurisotop (CEA, France) and $H_2{}^{18}O$ at 10% was from CEA-ORIS (France).

NMR at 9.4 T. Solutions of BSA and lysozyme were prepared by dissolving measured weights of the proteins in pure D_2O of known weight, with no further enrichment in $H_2{}^{17}O$. Preliminary measurements showed that this water is slightly enriched in ^{17}O. Samples (3 ml) were studied by ^{17}O NMR on a Bruker DPX400 spectrometer, in a 10-mm (i.d.) NMR tube, with a broadband probe, at 54.25 MHz. The 90° pulse length was 24 μs. All experiments were performed with an acquisition time set to at least 42 ms, corresponding to 512 points in the time domain, and a supplementary recovery delay of at least 5 ms. No proton decoupling was applied. The acquisition time was significantly larger than 5 T_1 but, because of the digital acquisition mode of the spectrometer, no detection was performed during the last 15 ms of the acquisition delay, and a supplementary delay was necessary before the next acquisition pulse. A one-pulse sequence enabled the magnitude of the signal to be estimated. The longitudinal relaxation times were determined with the inversion-recovery pulse sequence. T_2 measurements were performed with the Hahn-echo pulse sequence. The triple-quantum-filtered pulse sequences employed were those given in Eqs. [19] and [20], with the evolution delay τ_m kept to a minimum at 4 or 5 μs.

NMR at 11.7 T. Solutions of lysozyme were prepared by dissolving measured weights of the protein in a mixture of 80% $H_2{}^{18}O$ at 10% and 20% D_2O at 99.9% of known weight, with no further enrichment in $H_2{}^{17}O$. Probably because of its method of preparation, water enriched in ^{18}O was also enriched in ^{17}O. Hence, this mixture corresponded to water enriched in ^{17}O approximately five times more than at natural abundance. Three samples, of lysozyme concentrations of 10% (w/v), 15% (w/v), and 20% (w/v), respectively, were studied at 25 and/or 30°C before and after addition of tri-*N*-acetylglucosamine, $(NAG)_3$, a lysozyme inhibitor, added in excess (one and one-half times and twice the concentration of lysozyme for the two samples, respectively). The binding rate constant of $(NAG)_3$ to lysozyme is 1.3×10^2 s^{-1} at 45°C (*25*), and its binding constant is 1×10^5 M^{-1} (*26*). Thus, for the concentrations employed, almost all the lysozyme was complexed with $(NAG)_3$ and this complex was stable enough to be studied on its own by NMR. Some other solutions were prepared by dissolving measured weights of lysozyme in pure D_2O of known weight, added to 1% H_2O enriched at 10% in $H_2{}^{17}O$. Samples (0.6 ml) were studied by ^{17}O NMR on a Bruker DRX500 spectrometer, in a 5-mm (i.d.) NMR tube, with an inverse-detection broadband probe, at 67.80 MHz. The 90°

TABLE 1
Characteristics of Lysozyme Solutions at 20% (w/v) Studied at 9.4 and 11.7 T, as a Function of Temperature

Field	Temperature	R_{bulk} (s^{-1})	p_s ($\times 10^3$)	τ_s (ns)	$n_{water/prot}$	$R_1^{(1)}$ (s^{-1})	R_2 (s^{-1})
9.4 T[a]	25°C	243 ± 4	1.3 ± 0.05	4.8 ± 0.1	5.1 ± 0.2	349 ± 4	362 ± 1
	28°C	226 ± 4	0.95 ± 0.05	5.1 ± 0.1	3.8 ± 0.2	307 ± 4	330 ± 1
9.4 T	25°C	201 ± 2	1.2 ± 0.05	3.4 ± 0.1	4.3 ± 0.2	286 ± 2	312 ± 1
	30°C	184 ± 2	1.0 ± 0.05	3.3 ± 0.1	3.6 ± 0.2	245 ± 2	269 ± 2
	35°C	147 ± 2	0.95 ± 0.05	2.8 ± 0.1	3.5 ± 0.2	212 ± 2	147 ± 2
11.7 T	25°C	213 ± 2	1.1 ± 0.05	4.2 ± 0.1	4.4 ± 0.2	290 ± 2	236 ± 2
	30°C	185 ± 2	0.9 ± 0.05	4.0 ± 0.1	3.6 ± 0.2	248 ± 2	272 ± 2
	35°C	155 ± 2	1.05 ± 0.05	3.0 ± 0.1	4.1 ± 0.2	217 ± 2	240 ± 2

Note. All the samples were studied in (H_2O:D_2O) (4:1) except [a] for which the solvent was D_2O. R_{bulk} is the relaxation rate of bulk water in fast motion. p_s and τ_s are the fraction and correlation time of water in slow motion. $n_{s/prot}$ is the number of water molecules in slow motion per protein. $R_1^{(1)}$ is deduced from the values of R_{bulk}, p_s, and τ_s, via Eq. [18]. R_2 is the average transverse relaxation rate of water, measured via a Hahn echo.

pulse length was 14 μs. Other parameters were the same as at 9.4 T.

Processing. For samples where both transverse and longitudinal triple-quantum-filtered signals were analyzed, the processing was the same as in (*8*): the signals detected after the triple-quantum-filtered pulse sequences are proportional to $f_{31}^{(1)}(\tau_e) f_{31}^{(1)}(t_2)$ and $f_{31}^{(0)}(\tau_e) f_{31}^{(1)}(t_2)$ for transverse and longitudinal magnetization, respectively. The coefficients of proportion were deduced from the magnetization amplitude measured after the one-pulse sequence. The function $f_{31}^{(1)}(t)$ was then deduced from the "transverse" triple-quantum-filtered signal detected in the time domain for a given value of τ_e. The corresponding FID was transformed in an ASCII file and studied on a power Macintosh. The function $f_{31}^{(0)}(t)$ was studied by comparing the amplitude of the "longitudinal" and "transverse" triple-quantum-filtered signals after Fourier transformation. For this, the FIDs from the triple-quantum-filtered signals were zero filled to 512 points and an exponential line broadening of 20 Hz was applied prior to Fourier transformation.

Analysis. The value of the quadrupolar constant $(e^2qQ/h)(1 + \eta^2/3)^{1/2}$ was taken to be the same as that for D_2O ice: 6.5 MHz, following previous work performed by Denisov *et al.* (*5*). For given values of p_s and τ_s (the fraction and correlation time of water in slow motion), R_{bulk} was deduced from the longitudinal relaxation rate constant of water in Eq. [17]. The relaxation matrices $\mathbf{R}_{water}^{(n)}$ were then calculated and diagonalized. The time course of water magnetization after triple-quantum-filtered experiments was calculated, with its amplitude deduced from the intensity of the water signal after a one-pulse measurement (*8*). The parameters p_s and τ_s were then adjusted for an optimal correspondence between theory and experiment. This enabled the determination of the fraction of water in slow motion, its correlation time, and the relaxation rate R_{bulk} of water in fast motion and thereby the value of the relaxation rate $R_1^{(1)}$. The signal detected after a one-pulse sequence was also simulated, via the function $f_{11}^{(n)}(t)$, which is almost, but not exactly, exponential. It was then fitted by an exponential function, with a nonlinear curve fitting of the program Origin 3.5, so as to determine the expected value of the apparent relaxation rate of water transverse magnetization R_2^{sim}. The values of $R_1^{(1)}$ and R_2^{sim} were then compared to the apparent transversal relaxation rate of water effectively measured, R_2.

RESULTS AND DISCUSSION

Correlation between the Different Relaxation Rates Obtained

Aqueous solutions of lysozyme and BSA, of concentrations between 10 and 40% (w/v) and 8 and 15% (w/v), respectively, were studied at temperatures between 22 and 37°C, in water of two deuterium enrichments (25 and 100%). The corresponding parameters characterizing water in slow and in fast motion, deduced from T_1 measurements and transverse and longitudinal TQF signals, are given for typical samples in Tables 1 to 3, together with the calculated relaxation rate $R_1^{(1)}$ and the relaxation rate R_2 measured by the Hahn echo. One can note that for lysozyme, the number of water molecules in slow motion keeps close to 4, the expected value corresponding to buried water, as in (*24*), whatever the solvent and the magnetic field. For BSA, the number of water molecules in slow motion per protein keeps close to 30–40. This agrees with results obtained previously by ^{17}O and ^{1}H NMR (*8, 7*). On the contrary to lysozyme, these water molecules probably do not correspond to buried water. In the X-ray structure of human serum albumin (PDB accession code 1AO6 (*27*)), whose structure should be close to that of BSA, only 7 water molecules buried in the HSA dimer are detected. As a matter of fact, there are some hydrophobic pockets in the quaternary structure, where disordered water may be temporarily trapped but not detected by X ray (*6*). A similar phenomenon has already been observed in human interleukin-1β (*28*). In these samples, the value of $R_1^{(1)}$ deduced from R_{bulk}, p_s, and τ_s is systematically smaller than the

TABLE 2
Characteristics of Lysozyme Solutions of Different Concentrations in (H_2O:D_2O) (4:1) Studied at 11.7 T and at 30°C

Concentration % (w/v)	R_{bulk} (s^{-1})	p_s ($\times 10^3$)	τ_s (ns)	$n_{water/prot}$	$R_1^{(1)}$ (s^{-1})	R_2 (s^{-1})
15	172 ± 2	0.7 ± 0.05	3.4 ± 0.1	3.7 ± 0.3	221 ± 2	232 ± 1
20	185 ± 2	0.9 ± 0.05	4.0 ± 0.1	3.6 ± 0.2	248 ± 2	272 ± 1
23	201 ± 2	1.1 ± 0.05	4.5 ± 0.1	3.9 ± 0.2	291 ± 2	308 ± 1
30	220 ± 2	1.4 ± 0.05	5.4 ± 0.1	3.2 ± 0.2	331 ± 2	380 ± 1

Note. p_s, τ_s, R_{bulk}, $n_{water/prot}$, $R_1^{(1)}$, and R_2 have the same definitions as in Table 1.

average transverse relaxation rate of water R_2, measured by the Hahn echo. Because transverse relaxation of water should not be exactly monoexponential, the expected value of the apparent relaxation rate of water transverse magnetization R_2^{sim}, which describes the expected linewidth of ^{17}O-water if due only to quadrupolar relaxation, is slightly larger than $R_1^{(1)}$, but it is never more than 8 s^{-1} higher. It cannot explain the significant difference observed between R_2 and $R_1^{(1)}$ (Fig. 3), which reaches 100 s^{-1} for the BSA solution of larger viscosity (Table 3).

For the different samples studied, lysozyme at 9.4 and 11.7 T and BSA at 9.4 T, there is to a good approximation a linear correlation between R_2 and $R_1^{(1)}$ in the concentration and temperature ranges studied, when the solvent is either light or heavy water (Fig. 4). The characteristics of the regression curves, obtained by linear curve fitting of the data, are given in Table 4. One can see that for a given protein at a given field, there is a small but not always significant difference when the solvent is either H_2O or D_2O (Figs. 4b and 4c) and between the samples of sufficient concentration where an inhibitor is added or not (Fig. 4c). The difference between lysozyme and BSA, for a given field strength and in D_2O, seems to be slightly more important.

Origin of the Difference Observed between R_2 and $R_1^{(1)}$

The systematic important difference observed between R_2 and $R_1^{(1)}$ may be explained in two ways: a relaxation process other than quadrupolar relaxation, which would bring different contributions to transverse and longitudinal relaxation, and chemical exchange at an intermediate rate, which would enlarge significantly the linewidths. Scalar relaxation of the first kind would be due to the J couplings between ^{17}O and hydrogen in fast exchange between the water molecules. Its supplementary contribution to the transverse relaxation would be smaller than $J^2\tau_e S(S+1)/3$ (*29*), where τ_e is the rate of exchange of hydrogen, and S is its spin number. The coupling constant between ^{1}H and ^{17}O is 90 Hz in water whereas τ_e is smaller than 1.84 ms, its maximal value obtained in pure water (*30*). The corresponding contribution to the relaxation would then be smaller than 5 s^{-1}. It would be even shorter in deuterated water, where J is less than 14 Hz. Hence, this relaxation process could not explain the experimental results observed for either light or heavy water. Other phenomena, such as dilution of O_2 in the sample or hydrogen exchange between water and protein, could bring a contribution to the relaxation. But they should not be important in ^{17}O NMR (*7*).

The complementary contribution to R_2 should rather be due to the chemical exchange of water between different sites, where ^{17}O would have various chemical shifts. As the ^{17}O chemical shift range is quite large (more than 1000 ppm), chemical exchange may easily play a nonnegligible role in the apparent transverse relaxation of ^{17}O-water. Two possible origins of this phenomenon will be studied: (1) chemical exchange not fast enough between the different types of water and surface water, and (2) chemical exchange not fast enough between water in fast and in slow motion.

In the first hypothesis, the global longitudinal relaxation rate of water in fast motion can still be modeled as

TABLE 3
Characteristics of BSA Solutions at 80 and 150 g/L in D_2O Studied at 9.4 T, as a Function of Temperature

Concentration	Temperature	R_{bulk} (s^{-1})	p_s ($\times 10^3$)	τ_s (ns)	$n_{water/prot}$	$R_1^{(1)}$ (s^{-1})	R_2 (s^{-1})
80 g/L	25°C	226 ± 2	1.05 ± 0.05	6.8 ± 0.1	47 ± 3	327 ± 2	376 ± 1
	30°C	189 ± 2	0.8 ± 0.05	7.0 ± 0.1	35 ± 3	267 ± 2	307 ± 1
150 g/L	22°C	295 ± 2	1.75 ± 0.05	7.7 ± 0.1	43 ± 2	473 ± 2	572 ± 1
	25°C	268 ± 2	1.5 ± 0.05	8.5 ± 0.1	37 ± 2	429 ± 2	507 ± 1
	30°C	221 ± 2	1.3 ± 0.05	8.1 ± 0.1	32 ± 2	355 ± 2	398 ± 1
	35°C	184 ± 2	1.1 ± 0.05	7.0 ± 0.1	28 ± 2	294 ± 2	337 ± 1

Note. p_s, τ_s, R_{bulk}, $n_{water/prot}$, $R_1^{(1)}$, and R_2 have the same definitions as in Table 1.

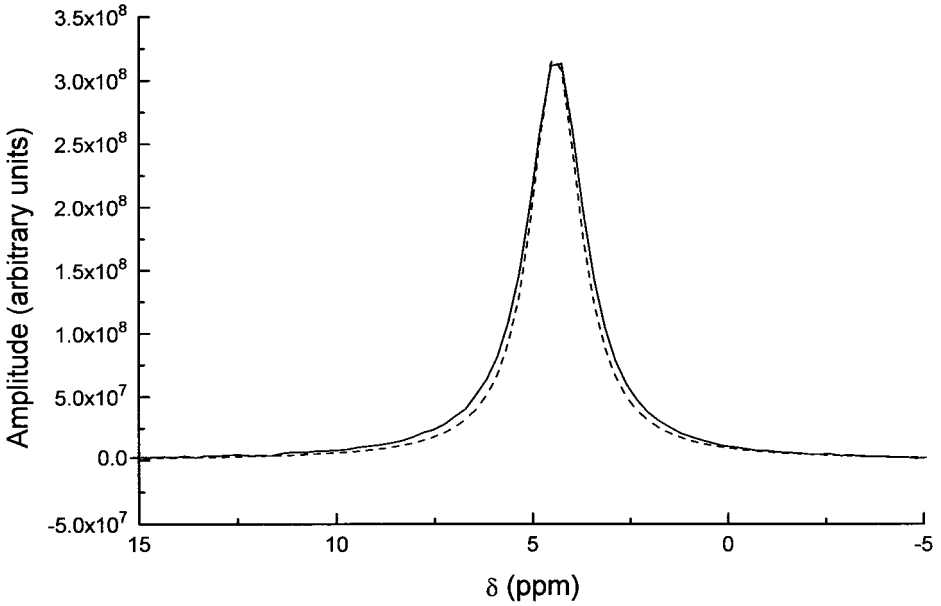

FIG. 3. Comparison of the NMR spectrum of ^{17}O-water in a lysozyme solution at 30% (w/v); $T = 30°C$, $B_0 = 11.7$ T (—) with the curve expected if the linewidth were due to quadrupolar relaxation only (- - -). The spectrum is almost a Lorentzian, whose linewidth corresponds to an apparent relaxation rate of 371 s^{-1}. The simulated curve has been calculated for fast exchange between two types of water, one in fast motion with a relaxation rate 208 s^{-1}, and one in slow motion, of fraction 0.168% and of correlation time 4.57 ns. These parameters were deduced from the longitudinal relaxation rate and from longitudinal and transverse TQF signals. The resulting curve is the Fourier transform of the triexponential $0.986 \exp(-327\,t) + 0.0037 \exp(-501\,t) + 0.01 \exp(-1173\,t)$. It is almost exponential, with the apparent relaxation rate $R_2^{\text{sin}} = 329\ s^{-1}$.

$$R_{\text{bulk}} = p_{\text{wb}} R_{\text{wb}} + (1 - p_{\text{wb}})\, R_{\text{free}}, \qquad [24]$$

where p_{wb} is the fraction of weakly bound water, R_{wb} is its relaxation rate, and R_{free} is the relaxation rate of pure water, whereas there is a supplementary contribution to transverse relaxation. Its exact value can be deduced from Eq. [11], where A represents pure water and B weakly bound water.

In the second hypothesis, the chemical exchange between water in slow and in fast motion is not fast enough, whereas it is for the different types of water in fast motion. As in the very fast exchange limit, if one neglects the multiexponential relaxation of water, the average longitudinal relaxation rate of water can be written

$$R_1 = R_1^{(0)} = p_s R_{1s} + (1 - p_s)\, R_{\text{bulk}}, \qquad [25]$$

where $R_{1s} = KA'$ of Eq. [6], the "apparent" relaxation rate of water in slow motion. Simultaneously, the transverse relaxation rate of water will be larger than the expected value,

$$R_1^{(1)} = p_s R_{2s} + (1 - p_s)\, R_{\text{bulk}}, \qquad [26]$$

with R_{2s} the "apparent" transverse relaxation rate of water in slow motion, equal to KP' of Eq. [9]. The exact value of the transverse relaxation rate can be deduced from Eq. [11], where A represents bulk water and B water in slow motion.

To find the origin of the observed contribution to transverse relaxation, simulations of chemical exchange for a system with properties similar to those studied in the experimental part are carried out. A lysozyme aqueous solution at 30% (w/v), at 35°C, studied at 9.4 T is considered. The fraction of water in slow motion is 0.12% and its correlation time is 4.9 ns. Its apparent transverse relaxation rate is then equal to $KA' = 88{,}000\ s^{-1}$. The expected global transverse relaxation time of water is 293 s^{-1} whereas the measured one is 342 s^{-1}. The difference of chemical shift between pure water and water in the lysozyme solution is 126 rad/s. First, the chemical exchange between two types of water in fast motion, pure water (A) and water weakly bound to lysozyme (B), is considered. There are approximately 500 water molecules weakly bound per protein (*10*). This corresponds to a fraction p_B equal to 0.2. The relaxation rate of pure water is $R_{2A} = 107\ s^{-1}$. That means that the relaxation rate of weakly bound water is $R_{2B} = 517\ s^{-1}$ and that the average transverse relaxation rate of bulk water is 245 s^{-1} instead of 189 s^{-1}, because of the chemical exchange between pure and weakly bound water. The problem is now to find adequate values of $\Delta\omega$ and k_B, so the real part of λ_+ of Eq. [11] is 245 s^{-1} and its imaginary part is 126 rad/s. The fast exchange limit corresponds to $\Delta\omega = 630$ rad/s and $k_B \geq 3 \times 10^6\ s^{-1}$. For smaller values of k_B, and/or larger values of $\Delta\omega$, the approximation of fast exchange is no longer valid and the real part of λ_+ may become larger than 189 s^{-1}. For example, if $\Delta\omega = 1200$ rad/s and $k_B = 1.3 \times 10^3\ s^{-1}$, $\lambda_+ = 249 + 126i$. This value of λ_+ is close to that detected for the lysozyme solution studied. Hence, the experimental result is possible if

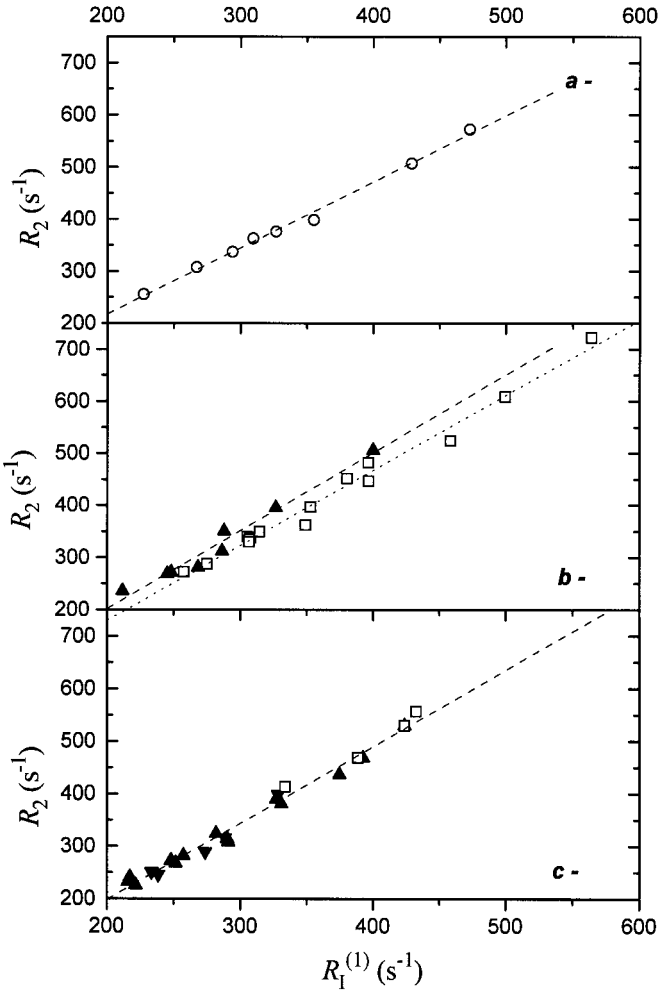

FIG. 4. Correlation between the relaxation rates $R_1^{(1)}$ and R_2 of water interacting with proteins. The value of $R_1^{(1)}$ was deduced from the study of transverse and longitudinal TQF signals together with the longitudinal relaxation rate of water. R_2 was the average transversal relaxation rate of water measured by a Hahn echo. Different solutions of BSA dissolved in D_2O were studied at 9.4 T (a). Lysozyme solutions in H_2O (▲) and D_2O (□) were also studied at 9.4 T (b) and 11.7 T (c). The samples studied at 11.7 T and where an inhibitor was added are symbolized as (▼).

there is chemical exchange at an intermediate rate between pure and weakly bound water, under the condition that the difference of chemical shift between pure and weakly bound water is about 3.5 ppm and the residence time of water near the protein surface is 0.8 ms. This value is much larger than the residence time of water near protein atoms which was estimated to less than 500 ps (*32*). In fact, these values do not correspond to the same phenomenon, as it is possible that a water molecule rapidly leaves a position close to a given protein atom but stays close to the protein surface for a while.

The second possibility is that there would be chemical exchange at an intermediate rate between water in fast (A) and in slow motion (B). Then, $p_B = 0.0012$, $R_{2A} = R_{bulk} = 189\ s^{-1}$, $R_{2B} = KA' = 88{,}000\ s^{-1}$ for the sample considered. The offset between the two populations cannot be estimated. The expected real value of λ_+ is 342 s^{-1}. The smaller value of $\Delta\omega$ for which it is obtained is 220,000 rad/s for $k_B = 4 \times 10^5\ s^{-1}$. This means that the chemical shift between water in slow and fast motion would be 645 ppm, which is theoretically possible but unlikely to happen, as the chemical shifts of OH groups are usually supposed to evolve in a range of 100 ppm (*33*).

From these simulations, it can be concluded that the more plausible hypothesis for explaining the observed results is that the chemical exchange between the different types of water in fast motion occurs at an intermediate rate and induces a supplementary contribution to transverse relaxation. This contribution reflects the long time weakly bound water spends close to the protein. This water probably corresponds to those described as a plasticizer in (*21*) and necessary to the enzymatic activity.

Finally, one can say that for characterizing water interacting with proteins, it is not possible to interpret directly its T_2 value measured by ^{17}O NMR as due only to quadrupolar relaxation. As a matter of fact, for samples of a given protein solution, there is a linear relationship between the measured relaxation rate R_2 and the relaxation rate $R_1^{(1)}$, expected if the transverse relaxation rate would be due to quadrupolar relaxation of water only. Consequently, for studying completely the properties of water interacting with given macromolecules, one has to perform a few calibration experiments where transverse and longitudinal relaxation are studied both with standard pulse sequences and after triple-quantum filters. The fraction and correlation time of water in slow motion and the relaxation rate of water in fast motion can then be deduced from the TQF experiments and from the longitudinal relaxation rate measurement. The theoretical value of the relaxation rate $R_1^{(1)}$, expected in the absence of any enlargement due to chemical exchange, is deduced from these three parameters. A relationship between R_2 and $R_1^{(1)}$ is then established. Then, for studying the properties of water interacting with macromolecules in another similar sample, it is sufficient to study the transverse and longitudinal relaxation rates of water together with its signal after a transverse triple-quantum filter. $R_1^{(1)}$ is deduced from R_2, using the curve drawn previously. Finally, the study of $R_1^{(1)}$ and $R_1^{(0)}$ and of the signal after a transverse triple-quantum filter enables the determination of the fraction and correlation time of water

TABLE 4
Parameters of the Regression Curves for the Fitting of $R_2 = A + B \times R_1^{(1)}$

Sample	Field	A	B	R	SD	P value
BSA (*8*)	9.4 T	−35.8	1.27	0.997	8.3	5.0×10^{-8}
Lyso-D_2O (*15*)	9.4 T	−108.8	1.44	0.993	15.5	2.1×10^{-13}
Lyso-H_2O (*6*)	9.4 T	−97.8	1.50	0.986	15.9	6.86×10^{-6}
Lyso (*26*)	11.7 T	−93.17	1.46	0.993	12.7	1.9×10^{-23}

Note. BSA represents bovine serum albumin dissolved in D_2O and Lyso, lysozyme dissolved in either H_2O or D_2O, eventually containing an inhibitor.

TABLE 5
Win of Time When the T_2 Measurement Is Used in Place of Longitudinal TQF Relaxation Analysis, for Characterizing Water Interacting with Proteins by ^{17}O NMR

			Time spent per measurement				
Sample	Field	Solvent	T_1	T_2	TTQF	LTQF	Win of time
BSA (80 g/L)	9.4 T	D_2O	15 min	15 min	11 h 30	23 h	65%
BSA (150 g/L)	9.4 T	D_2O	15 min	15 min	5 h 45	23 h	79%
Lyso (30%, w/v)	9.4 T	D_2O	15 min	15 min	5 h 45	23 h	79%
Lyso (15%, w/v)	11.7 T	H_2O[a]	2 min	2 min	3 h 45	15 h	80%

[a] The sample was slightly ^{17}O enriched compared to those where D_2O was employed.

in slow motion, together with the intrinsic relaxation rate of water in fast motion. Once the calibration is performed, this enables a significant win of time (Table 5). It is also interesting to note that the difference observed between R_2 and $R_1^{(1)}$ should bring information concerning the residence time of weakly bound water in the vicinity of the protein.

Consequences on ^{17}O-Water Triple-Quantum Analysis

The comparison of the experimental results with the simulations means that the chemical exchange between pure and weakly bound water is not very fast and that the transverse and longitudinal relaxation rates of bulk water are unequal. The transverse relaxation matrix of bulk water is then different from its longitudinal relaxation matrix, which will stay equal to $\mathbf{R}_{bulk}$. We will call the transverse relaxation matrix of bulk water $\mathbf{R}_{bulk}^{(1)}$. It is diagonal, because bulk water is in fast motion. In it, the relaxation rates of triple and fifth coherences should be modified compared to those in the matrix $\mathbf{R}_{bulk}$, in the same way as for the single-quantum coherence. At a matter of fact, for these coherences, the offsets between pure and weakly bound water are $3\Delta\omega$ and $5\Delta\omega$, respectively. Then, for the estimated value of k_B (about 1.3×10^3 s^{-1}), the chemical exchange between the different types of water is in the very fast exchange limit. Finally, the diagonal terms of the relaxation matrix $\mathbf{R}_{bulk}^{(1)}$ are $\{R_{bulk} + \Delta R;\ 33/8\ R_{bulk};\ 15/8\ R_{bulk}\}$, where ΔR is a supplementary contribution to transverse relaxation, due to chemical exchange. This new matrix $\mathbf{R}_{bulk}^{(1)}$ should be used in place of $\mathbf{R}_{bulk}$ in Eq. [15], for the study of transverse magnetization behavior. In fact, this does not change significantly the results of the analysis. For the sample of lysozyme 30% (w/v) studied in the simulations, the fraction of water in slow motion and the relaxation rate of water in fast motion are almost the same in the two cases. The only parameter modified is the correlation time of water in slow motion which is 0.2 ns higher when the matrix $\mathbf{R}_{bulk}^{(1)}$ is used. Thus, it can be concluded that it is not necessary to introduce the relaxation matrix $\mathbf{R}_{bulk}^{(1)}$ to analyze ^{17}O-water by triple-quantum-filtered sequences, but that the correlation time of water in slow motion will then be slightly underestimated.

Estimation of the Systematic Errors Due to the Approximations Made

Lysozyme at 30% (w/v) in D_2O is first analyzed at 9.4 T and 25°C as in previous studies (*8, 24*): the parameters R_{bulk}, p_s, and τ_s and hence $R_1^{(1)}$ are deduced from the values of $R_1^{(0)}$ and transverse and longitudinal TQF signals. It is found that the fraction of water in slow motion is 0.187% and its correlation time is 5.20 ns. The calculated relaxation rate $R_1^{(1)}$ is then 446.15 s^{-1}. This value of $R_1^{(1)}$, together with the relaxation rate $R_1^{(0)}$ and the transverse triple-quantum-filtered signal, is then used as initial data for the program developed in this work. The optimal values of p_s and τ_s deduced from these data are 0.180% and 5.25 ns, respectively. The small differences found between the two methods of analysis are due to the approximations made on water relaxation in the program. They should not be significant compared to the precision of the measurement, but need not be neglected if a more precise result is expected.

CONCLUSION

The simultaneous analysis of data from transverse triple-quantum-filtered NMR experiments and conventional relaxation rate measurements at a given field strength enables the number of water molecules in slow motion, together with their average correlation time, to be determined, at the expressed condition that a few calibration experiments have been performed previously. This calibration is necessary for the quantification of the line enlargement of water, due to the chemical exchange between free water and water weakly interacting with the protein. The method developed should enable the study of various samples more rapidly, as the time-consuming longitudinal triple-quantum-filtered experiment does not need to be performed on all of them. Also, it does not need preliminary knowledge of the correlation time of water in slow motion for adequate results to be given.

For higher precision, the calibration experiments should be performed on similar samples: with the same proteins dissolved in water of a similar deuterium enrichment and at the same field strength. It is interesting to note that no further calibration measurement needs to be performed for the addi-

tional study of a small molecule, as an inhibitor, interacting with the protein. This should bring good perspectives for biochemical studies. The calibration performed also enables the estimation of the contribution of chemical exchange to the transverse relaxation of water in fast motion, and hence the residence time of weakly bound water in the vicinity of the protein. Thanks to this information, a better picture of water weakly interacting with the proteins should be obtained. As a matter of fact, complementary measurements should be performed to validate the value of the very long residence time obtained here.

ACKNOWLEDGMENTS

Michel Trierweiler and Françoise Mabon are thanked for assistance with the NMR spectrometer.

REFERENCES

1. F. C. Colombo, D. C. Rau, and V. A. Parsegian, Protein solvation in allosteric regulation: A water effect on hemoglobin, *Science* **256,** 655–659 (1992).
2. K. Takano, J. Funahashi, Y. Yamagata, S. Fujii, and Y. Katsuhide, Contribution of water molecules in the interior of a protein to the conformational stability, *J. Mol. Biol.* **274,** 132–142 (1997).
3. G. Otting, E. Liepinsh, and K. Wüthrich, Protein hydration in aqueous solution, *Science* **254,** 974–980 (1991).
4. V. P. Denisov and B. Halle, Hydrogen exchange and protein hydration: The deuteron spin relaxation dispersions of bovine pancreatic trypsin inhibitor and ubiquitin, *J. Mol. Biol.* **245,** 298–709 (1995).
5. V. P. Denisov and B. Halle, Protein hydration dynamics in aqueous solution: A comparison of bovine pancreatic trypsin inhibitor and ubiquitin by oxygen-17 spin relaxation dispersion, *J. Mol. Biol.* **245,** 682–697 (1995).
6. V. P. Denisov and B. Halle, Protein hydration dynamics in aqueous solution, *Faraday Discuss.* **103,** 227–244 (1996).
7. S. Kiihne and R. G. Bryant, Protein-bound water molecules counting by resolution of ^{1}H spin–lattice relaxation mechanisms, *Biophys. J.* **78,** 2163–2169 (2000).
8. E. Baguet, B. E. Chapman, A. M. Torres, and P. W. Kuchel, Determination of the bound water fraction in cells and protein solutions using ^{17}O-water multiple-quantum filtered relaxation analysis, *J. Magn. Reson. B* **111,** 1–8 (1996).
9. E. Baguet, N. Hennebert, B. E. Chapman, A. M. Torres, and P. W. Kuchel, Mobility of water in biological systems studied by ^{17}O NMR via multiple-quantum filtered relaxation analysis, *Magn. Reson. Chem.* **35,** S47–S51 (1997).
10. A. M. Torres, S. M. Grieve, B. E. Chapman, and P. W. Kuchel, Strong and weak binding of water to proteins studied by NMR triple-quantum filtered relaxation spectroscopy of ^{17}O-water, *Biophys. Chem.* **67,** 187–198 (1997).
11. A. M. Torres, S. M. Grieve, and P. W. Kuchel, NMR triple-quantum filtered relaxation analysis of ^{17}O-water in insulin solutions: An insight into the aggregation of insulin and the properties of its bound water, *Biophys. Chem.* **70,** 231–239 (1998).
12. S. M. Grieve, B. Wickstead, A. M. Torres, P. Styles, S. Wimperis, and P. W. Kuchel, Multiple-quantum filtered ^{17}O and ^{23}Na NMR analysis of mitochondrial suspensions, *Biophys. Chem.* **73,** 137–143 (1998).
13. S. H. Koenig, K. Hallenga, and M. Shporer, Protein–water interaction studied by solvent ^{1}H, ^{2}H and ^{17}O magnetic relaxation, *Proc. Natl. Acad. Sci. USA* **72,** 2667–2671 (1975).
14. B. Halle, T. Andersson, S. Forsén, and B. Lindman, Protein hydration from water oxygen-17 magnetic relaxation, *J. Am. Chem. Soc.* **103,** 500–508 (1981).
15. G. Jaccard, S. Wimperis, and G. Bodenhausen, Multiple-quantum NMR spectroscopy of $S = 3/2$ spins in isotropic phase: A new probe for multiexponential relaxation, *J. Chem. Phys.* **85,** 6282–6293 (1986).
16. C.-W. Chung and S. Wimperis, Measurement of spin-5/2 relaxation in biological and macromolecular systems using multiple-quantum NMR techniques, *Mol. Phys.* **76,** 47–81 (1992).
17. J. S. Leigh, Jr., Relaxation times in system with chemical exchange: Some exact solutions, *J. Magn. Reson.* **4,** 308–311 (1971).
18. R. Freeman, Chemical exchange, *in* "A Handbook of Nuclear Magnetic Resonance," pp. 28–32, Longman, Essex, Great Britain (1987).
19. T. E. Bull, Nuclear magnetic relaxation of spin-3/2 nuclei involved in chemical exchange, *J. Magn. Reson.* **8,** 344–353 (1972).
20. C. C. F. Blake, W. C. A. Oulford, and P. J. Artymiuk, X-ray studies of water in crystals of lysozyme, *J. Mol. Biol.* **167,** 693–723 (1983).
21. S. Bone and R. Pethig, Dielectric studies of protein hydration and hydration-induced flexibility, *J. Mol. Biol.* **181,** 323–326 (1985).
22. B. Halle and H. Wennerström, Nearly exponential quadrupolar relaxation. A perturbation treatment, *J. Magn. Reson.* **44,** 89–100 (1981).
23. R. R. Ernst, G. Bodenhausen, and A. Wokaun, "Principles of Nuclear Magnetic Resonance in One and Two Dimensions," pp. 257–261, Oxford Univ. Press, Oxford (1987).
24. E. Baguet and N. Hennebert, Characterisation by triple-quantum filtered ^{17}O-NMR of water molecules buried in lysozyme and trapped in a lysozyme-inhibitor complex, *Biophys. Chem.* **77,** 111–121 (1999).
25. C. M. Dobson, The structure of lysozyme in solution, *in* "NMR in Biology" (R. A. Dwek, I. D. Campbell, R. E. Richards, and R. J. P. Williams, Eds.), pp. 63–94, Academic Press, London (1977).
26. S. Kuramitsu, K. Ikeda, K. Hamaguchi, S. Miwa, and T. Nishina, Interactions of *N*-acetyl-chitooligosaccharides with human and hen lysozymes, *J. Biochem.* **72,** 1109–1115 (1972).
27. S. Sugio, A. Kashima, S. Mochizuki, M. Noda, and K. Kobayashi, Crystal structure of human serum albumin at 2.5 A resolution, *Protein Eng.* **12,** 439–446 (1999).
28. J. A. Ernst, R. T. Clubb, H.-X. Zhou, A. M. Gronenborn, and G. M. Clore, Demonstration of positionally disordered water within a protein hydrophobic cavity by NMR, *Science* **267,** 1813–1817 (1995).
29. A. Abragam, "Les principes du magnétisme nucléaire," Presses Universitaires de France, Paris, France (1961).
30. S. Meiboom, Nuclear magnetic resonance study of the proton transfer in water, *J. Chem. Phys.* **34,** 375–388 (1961).
31. C. Guillou, Ph.D. thesis, Application de la mesure du fractionnement isotopique de l'hydrogène à la détection de l'enrichissement des vins, Nantes (1986).
32. R. M. Brunne, E. Liepinsh, G. Otting, K. Wüthrich, and W. F. van Gunsteren, Hydration of proteins—A comparison of experimental residence times of water molecules solvating the bovine pancreatic trypsin inhibitor with theoretical model calculations, *J. Mol. Biol.* **231,** 1040–1048 (1993).
33. I. P. Gerothanassis, Oxygen-17 NMR, *in* "Encyclopedia of Nuclear Magnetic Resonance," Vol. 5, pp. 3430–3440, Wiley, Chichester, England (1996).